Object-oriented computational framework for the simulation of variably saturated flow in soils, using a reduced complexity model

Grigorios G. Anagnostopoulos*

Institute of Environmental Engineering, ETH Zurich, 8093 Zurich, Switzerland

Paolo Burlando*

Institute of Environmental Engineering, ETH Zurich, 8093 Zurich, Switzerland

Abstract

A simple and efficient computational modelling framework is presented for the simulation of variably saturated flows in porous media, which is not based on a conventional numerical solution of the Richards' equation. The computational domain is discretized with a regular grid and simple rules govern the flow dynamics. Each cell can have distinct hydraulic properties and its state depends only on the state of its neighbouring cells. These concepts make easier and computationally more efficient the simulation of large-scale variably saturated flow in heterogeneous media. Due to its object oriented design, the presented framework is very flexible and easily extensible and can be used for various engineering applications (e.g. prediction of rainfall-induced landslides, water and solute transport in agricultural soils), where the simulation of variably saturated flow is crucial. The modelling framework has been validated with experimental results and analytical solutions for 2-D and 3-D problems available from the literature, showing very good agreement even in cases where strong non linearities existed.

Keywords: large scale problems, heterogeneous media, macroscopic cellular

*Corresponding author

Email addresses: anagnostopoulos@ifu.baug.ethz.ch (Grigorios G. Anagnostopoulos), burlando@ifu.baug.ethz.ch (Paolo Burlando)

automata, object- oriented framework, simulation

1. Introduction

Numerical simulation of flow in the vadose zone still constitutes a challenging issue, even though numerous approaches and schemes have been presented in the last decades. The partial differential equation describing flow in partially saturated porous media, Richards' equation (Richards, 1931), is highly non linear due to pressure head dependencies in the specific soil water capacity and the relative hydraulic conductivity terms. Its mathematical behaviour changes according to the flow conditions encountered in the problem under consideration. When capillary forces are the driving forces of the flow phenomenon the equation has a non linear parabolic character. On the other hand, in flow regimes where the gravitational forces dominate over the capillary forces the equation turns into an hyperbolic equation. Furthermore, once fully saturated conditions are reached Richards' equation transforms to its simplest form, which is a linear elliptic equation. The most challenging issue in real-world simulations lies in the fact that all the above aforementioned scenarios can be combined, thus rendering the choice of its appropriate numerical treatment very difficult. Richards' equation can be written in three different mathematically equivalent forms, the numerical treatment of which is, however, substantially different. These forms are shown in Table 1, where $C(h) = \frac{\partial \theta}{\partial h}$ is the specific soil water capacity and $D(\theta)$ is the diffusivity.

Not all the forms of the Richards' equation are appropriate, in terms of mass balance errors and convergence ability, for all the simulation scenarios. The h-based form is inappropriate for highly non-linear problems (e.g. infiltration into very dry heterogeneous soil) due to its poor mass conservation performance, while the θ-based form cannot be used for fully saturated conditions. The mixed h-θ-based form combines both decent mass-conservation performance and computational efficiency (Celia et al., 1990). Finite differences (Clement et al., 1994; van Dam and Feddes, 2000), finite volumes (Manzini and Ferraris, 2004;

McBride et al., 2006) and finite elements methods (Šimůnek et al., 2008; Fahs et al., 2009) are the most widely used methods to descretize all three forms of Richards' equation. Most of them involve an iteration scheme (e.g. Picard, Newton, Newton-Krylov, fast-secant and relaxation methods) in order to deal with the non linear nature of the equation. Finite differences methods are used in the majority of the one dimensional models, while finite volume and finite elements methods are used in two and three dimensional models. Most of the numerical techniques developed so far, which are based on the discretization of the partial differential equation, lead inevitably to complex and computationally expensive algorithms especially for large-scale problems, where the presence of strong non linearities and complex boundary conditions are evident. In order to circumvent these difficulties researchers used special transformations (Williams et al., 2000), which reduce the non linearity of the initial equation, and switching methods (Sadegh Zadeh, 2011), which switch between the mixed-based form (mass conservative but only applicable in unsaturated conditions) and the h-based (pressure-based) form (appropriate for both saturated and unsaturated conditions). Although a lot of progress was made towards more efficient modelling, most of the algorithms are limited to computational grids of reduced dimension and small time steps in order to prevent numerical instability.

The difficulties and the limitations posed by the aforementioned methods led some researchers to change direction and stop considering the numerical integration of Richards equation as a corner-stone for the simulation of variably saturated flow. Models based on Cellular Automata (CA) are one of these alternative directions that many researchers investigated. The concept of CA was introduced by von Neumann (1966) and was extended by Wolfram (Wolfram, 1986, 1994). It is based on an inherently discrete idealization of the physical system, whose domain is divided into cells having the same shape. Each cell is characterized by a set of parameters describing as accurately as possible its physical condition. These parameters constitute the state of each cell, which is updated through a fixed update function (local transition function) by taking into account the states of the neighboring cells. The state update can be

synchronous or asynchronous but can be done only at discrete time steps. One of the greatest advantages of CA framework is that the modelling is performed in an inherent parallel way because the transition function is applied simultaneously to all cells and the state of each cell depends only on the state of its neighbouring cells. This fact can facilitate enormously the execution in parallel systems with many threads and allows the increase of spatial and temporal domains of simulations while the computational time is still kept to acceptable levels.

Lattice Gas Automata (LGA) and Lattice Boltzmann Methods (LBMs) are two of the most important applications of the CA framework. LGA models describe the flow motion by introducing a regular lattice where each cell is connected to its neighbours. The state of each cell is purely boolean (boolean particle number) and represents the presence or non presence of a particle within the cell (Frisch et al., 1987). After a time step interval, each particle moves to a neighbouring cell. When more than one particle arrive at the same cell, some fixed collision rules, which respect the mass and momentum conservation, make them collide and change directions. The density at a cell can be calculated by counting the number of particles at each cell. If the particles are multiplied with the unitary velocity before being summed, the momentum at the cell can be obtained. The main disadvantage of LGA is that a lot of statistical noise is introduced in the computation of density, momentum and velocity for individual cells, and for this reason averaging over larger region should be carried out in order to obtain reasonably noise-free results.

LBMs was developed in order to overcome the LGA limitations, namely to remove the statistical noise by replacing the boolean particle number with its corresponding ensemble average, the so-called density distribution function (McNamara and Zanetti, 1988; Succi et al., 1991). LBMs have several advantages over the conventional computational fluid dynamics methods, which solve numerically, the Navier-Stokes equations, especially in the presence of complex boundaries, incorporating microscopic interactions and parallelization of the algorithm. In addition, both LGA and LBM converge at the limit to Navier-Stokes

equations for incompressible fluids (Chen et al., 1992; Qian et al., 1992).

Although the application of LGA and LBM was until now primarily confined to microscopic scale applications (Sukop and Or, 2004; Zhang et al., 2005; Chau et al., 2005), their importance for computational fluid dynamics is indisputable. The need for the simulation of macroscopic flow phenomena led to the use of macroscopic CA models that deal directly with the macroscopic variables, which describe the evolution of the physical system examined. A large number of studies dealing with various physical problems were carried out under this framework. Lava flows (Rongo et al., 2008), debris flows (D' Ambrosio et al., 2007), groundwater modelling (Ravazzani et al., 2011), snow avalanches (Barpi et al., 2007) and river deltas formation (Seybold et al., 2009) are some examples of the diverse problems that were tackled within this framework. However, in most of the above applications, the transitions functions are based on parameters that do not have a clear physical meaning and, as a consequence, calibration is needed to assess the best parameter range.

An example of macroscopic CA model, which uses a transition function based on physical law, is that of Mendicino et al. (2006), who modeled unsaturated flow in soils using Darcy's law as transition function. In this way the parameters used for the characterization of each cell have a physical meaning, thus avoiding the necessity of introducing fictitious parameters. The main drawback of their approach is that the time step depends directly on the spatial grid and the hydraulic properties of the cells, obeying a specific condition for the algorithm to be convergent. This restriction can increase the computational burden dramatically when large scale problems are examined with unfavorable soil hydraulic properties and boundary conditions, which is often the case in catchment hydrology.

In this paper we present a computational framework which extends the concepts introduced in Mendicino et al. (2006) and is based on the macroscopic CA approach for the simulation of variably saturated flow in heterogeneous soils. An object-oriented design is followed, through which the description of the various processes is straightforward, thus allowing to create a flexible and reusable

model structure. It can be used as the core of a more complex large-scale model for the simulation of various phenomena by incorporating some additional components (e.g evapotranspiration, surface runoff routing, hysteresis in soil water retention curve) with minimal effort. Possible areas of application can be found in all engineering disciplines where the simulation of the soil water budget is essential, and particularly for the prediction of rainfall-triggered landslides and water and solute transport in agricultural soils.

The computational algorithm used is proved to be unconditionally stable, which makes the selection of the time step independent of the grid size and the cell hydraulic properties. However, the convergence of the algorithm alone does not guarantee that the mass balance errors and the accuracy are kept in acceptable levels, especially in cases when the strong non linearities exist (very dry and near saturation conditions). An iteration procedure combined with an efficient (in terms of accuracy and computational burden) convergence criterion (Huang et al., 1996) is used to handle efficiently these cases. We use Soil Water Retention Curves (SWRC) that follow the classical van Genuchten model (VG, van Genuchten and Nielsen (1985), as well as some modified VG models that improve the accuracy and convergence at the cells near saturation (Vogel et al., 2001; Ippisch et al., 2006; Schaap and van Genuchten, 2005) and the Brooks and Corey model (Brooks and Corey, 1964). Furthermore, the performance of various approximations for the internodal conductivities is investigated. The best results were achieved by a model that is based on the steady state distribution of the potential head and distinguishes between three major cases of the shape of the head profile (Szymkiewicz, 2009). Finally, the model is tested against 2-D infiltration and drainage experimental data in homogeneous and heterogeneous soils and against a 3-D analytical solution for simple boundary and initial conditions.

2. Methods

2.1. Structure and development of the computational framework

Hydrological modelling is dominated by procedure-oriented languages, such as FORTRAN and C. Object-Oriented Programming (OOP) opened new horizons for better description and more effective modelling of complex hydrological phenomena. The most widely used object-oriented language is C++, although Java and Python are also used in scientific applications. OOP can become a very efficient tool in environmental engineering applications because it makes easier the development of a flexible, reusable and easily extendable code.

In the development of our framework we are making use of all the OOP features of C++. A flow chart, which shows the class structure of our model, is presented in Figure 1. The class *initializeSim* contains the methods to read all the parameters and input files that are necessary for the simulation, initializes all the objects needed for the simulation and creates the discretized computational domain, taking into account the boundary conditions and sets up the initial conditions of the problem. Each process we want to incorporate in our framework is represented by a separate class: class *subsurfComp* computes the subsurface flow, class *surfComp* computes the surface flow, while additional classes represent other processes that could be important for the phenomenon under study (e.g. evapotranspiration, hysteresis in soil water retention curve). Special class hierarchies are also created to describe the different Soil Water Retention Curves (SWRC) and the different methods of averaging the inter-nodal conductivity, the objects of which are instantiated within the class that controls the subsurface flow. The class *globalSimulation* combines all the process-objects and runs the transition function on all the cells of the computational domain. It also controls the iteration procedure in order to obtain a user-defined level of accuracy and also contains an adaptive time-stepping routine, which adjusts the time step of the simulation according to the number of iterations.

2.2. Computational procedure

According to the macroscopic CA notion the computational domain consists of a two or three dimensional lattice, which is composed by rectangular or prismatic cells respectively. Spatial heterogeneity can be tackled effectively because each cell can have its own constitutive hydraulic properties. At each cell we compute the pore water pressure, the field of which is assumed to be continuous but not necessarily differentiable. The definition of variably saturated flow problem requires the determination of initial and boundary conditions. The boundary conditions can be of two kinds: on some parts of the boundary the hydraulic head can be prescribed (Dirichlet's boundary conditions), while on some other parts a prescribed flow rate is specified (Neumann's boundary conditions).

We assume that every cell of the lattice communicates with its neighbours only through its faces as it is shown in Figure 2. The volumetric flow rate, Q_{ac}, through each face is computed using the Darcy-Buckingham's law

$$Q_{\alpha c} = \overline{K}_{\alpha c} \left(\frac{H_\alpha - H_c}{l_{\alpha c}} \right) A_{\alpha c}, \tag{1}$$

where the subscript α represents the neighbouring cell that is adjacent to the α-th face of the cell c, $\overline{K}_{\alpha c}$ is the averaged inter-cell conductivity $[L/T]$, H_α and H_c are the total heads of the cells $[L]$ given by the sum of the pressure head and the elevation of the cell, $l_{\alpha c}$ is the cell dimension $[L]$ and $A_{\alpha c}$ is the area through which the inter-cell mass flow passes $[L^2]$. If the cell has some faces that are adjacent to the domain‘s boundary and a Neumanns condition is prescribed to that part of the boundary then $Q_{\alpha c} = Q^{\alpha}_{bound}$.

The mass balance equation must be satisfied for each cell of the lattice. Coupling the discrete formulation of the mass balance of an arbitrary cell with the constitutive equation (1) yields the following equation

$$\sum_{\alpha \in I} \overline{K}_{\alpha c} \left(\frac{H_\alpha - H_c}{l_{\alpha c}} \right) A_{\alpha c} + \sum_{\alpha \in I'} Q^{\alpha}_{bound} + S_c = V_c \sigma(h_c) \frac{\Delta H_c}{\Delta t}, \tag{2}$$

where I is the domain of the faces of the cell which are adjacent to a neighbouring cell, I' is the domain of the faces which are adjacent to boundary of the entire

domain, S_c is a source-sink term $[L^3T^{-1}]$, V_c is the cell volume $[L^3]$, h_c is the pressure head, which is expressed as the ratio between the capillary pressure p_c $[ML^{-1}T^{-2}]$ and the specific weight of liquid γ_w $[ML^{-2}T^{-2}]$, and $\sigma(h_c)$ is the specific volumetric storativity $[L^{-1}]$.

The specific volumetric storativity $\sigma(h_c)$ can be defined in the whole pressure domain as follows

$$\sigma(h_c) = C_c(h_c) + S_e(h_c)S_s, \tag{3}$$

where $C_c(h_c) = \Delta\theta_c/\Delta h$ is the specific soil water capacity, $S_e = (\theta(h_c) - \theta_r)/(\theta_s - \theta_r)$, θ_r is the residual water content and θ_s is the saturated water content. S_s represents the specific volumetric storage, which is the volume of water that a unitary volume of the saturated system releases from the storage under a unitary decline in pressure head and depends on the compressibility of the porous medium and on the compressibility of the fluid.

At the right-hand side of Equation (2) the term $C_c(h_c)\frac{\Delta H_c}{\Delta t}$ is highly non linear due to the non linear nature of the specific soil water capacity. In order to achieve better mass conservation for various sizes of spatial grids and time steps we adopt the approach followed by Celia et al. (1990) and the right-hand side of Equation (2) takes the following form

$$\begin{aligned} V_c\left(C_c(h_c)\frac{\Delta H_c}{\Delta t} + S_e(h_c)S_s\frac{\Delta H_c}{\Delta t}\right) = \\ = V_c\Big(\frac{\theta_c^{t+\Delta t,m} + C_c^{t+\Delta t,m}(H_c^{t+\Delta t,m+1} - H_c^{t+\Delta t,m}) - \theta_c^t}{\Delta t} + \\ + S_e^{t+1/2}S_s\frac{H_c^{t+\Delta t,m+1} - H_c^t}{\Delta t}\Big), \end{aligned} \tag{4}$$

where m denotes the level of iteration and $S_e^{t+1/2} = \frac{S_e^{t+\Delta t,m} + S_e^t}{2}$.

Equation (2) is applied in all the cells of the lattice except those, which have a Dirichlet boundary condition, the hydraulic head of which is fixed throughout the simulation. In order to determine the total head $H_c^{t+\Delta t}$ and the pressure head $h_c^{t+\Delta t}$ at the time $t + \Delta t$ we write Equation (2), taking into account Equation (4), for the generic cell c for the time interval $[t, t + \Delta t]$ and we solve for $H_c^{t+\Delta t}$, that is

$$\sum_{\alpha\in I}\overline{K}_{\alpha c}\left(\frac{H_\alpha^{t+\Delta t,m}-H_c^{t+\Delta t,m+1}}{l_{\alpha c}}\right)A_{\alpha c}+\sum_{\alpha\in I'}Q_{bound}^{\alpha}+S_c=$$
$$=V_c\Big(\frac{\theta_c^{t+\Delta t,m}+C_c^{t+\Delta t,m}(H_c^{t+\Delta t,m+1}-H_c^{t+\Delta t,m})-\theta_c^t}{\Delta t}+$$
$$+S_e^{t+1/2}S_s\frac{H_c^{t+\Delta t,m+1}-H_c^t}{\Delta t}\Big)\Leftrightarrow$$
$$\Leftrightarrow H_c^{t+\Delta t,m+1}=\frac{\sum_{\alpha\in I}\frac{\overline{K}_{\alpha c}A_{\alpha c}}{l_{\alpha c}}H_\alpha^{t+\Delta t,m}+\sum_{\alpha\in I'}Q_{bound}^{\alpha}}{\sum_{\alpha\in I}\frac{\overline{K}_{\alpha c}A_{\alpha c}}{l_{\alpha c}}+\frac{V_c}{\Delta t}(C_c^{t+\Delta t,m}+S_e^{t+1/2}S_s)}+$$
$$+\frac{\frac{V_c}{\Delta t}(C_c^{t+\Delta t,m}H_c^{t+\Delta t,m}-\theta_c^{t+\Delta t,m}+\theta_c^t+S_e^{t+1/2}S_sH_c^t)+S_c}{\sum_{\alpha\in I}\frac{\overline{K}_{\alpha c}A_{\alpha c}}{l_{\alpha c}}+\frac{V_c}{\Delta t}(C_c^{t+\Delta t,m}+S_e^{t+1/2}S_s)},\qquad(5)$$

It is proved in the Appendix that using Equation (5) the computational scheme is convergent irrespective of the choice of the time step Δt and the cell size $l_{\alpha c}$. We also investigated the convergence of the algorithm numerically by running the infiltration experiment of Vauclin et al. (1979) (see section 3.1) for various spatial grid sizes. As it is shown in Figure 3 the proposed algorithm converges to a solution that is very good for all grid sizes and becomes closer to the experimental data as the spatial discretization is getting finer. Another advantage of the above formulation is that the computation of the value of the total head $H_c^{t+\Delta t,m+1}$ of one cell depends only on values that are known from the previous iteration level, thus avoiding to solve a large system of equations (which is the basic characteristic of all implicit schemes with a Picard-type formulation) and making the scheme suitable for parallel computing.

2.3. Soil Water Retention Curves

The computation of the hydraulic head cannot be carried out unless we specify the non-linear relation between the pressure head h and the hydraulic conductivity $K(h)$ and that between the water content $\theta(h)$ and the specific soil water capacity $C_c(h)$, which are expressed by the Soil Water Retention Curves (SWRC). There are numerous models in the literature for the determination of

the SWRC. The most widely used model is the van Genuchten - Mualem model (van Genuchten and Nielsen, 1985), which is given by the following equations,

$$S_e = \begin{cases} [1 + (\alpha|h|)^n]^{-m}, & \text{for } h < 0 \\ 1, & \text{for } h \geqslant 0 \end{cases} \tag{6}$$

$$K(h) = \begin{cases} S_e^b \left[1 - \left(1 - S_e^{1/m}\right)^m\right]^2 K_{sat}, & \text{for } h < 0 \\ K_{sat}, & \text{for } h \geqslant 0, \end{cases} \tag{7}$$

where $S_e = (\theta - \theta_r)/(\theta_s - \theta_r)$, θ_r is the residual water content, θ_s is the saturated water content and n, α, $m = 1 - 1/n$ and b are empirical shape parameters. Although equations (6) and (7) found widespread use, several discussions appeared in the literature concerning of their limits of validity. For instance, it was shown (Vogel et al., 2001; Ippisch et al., 2006) that conductivities derived from the van Genuchten - Mualem model can be quite sensitive to the shape of the SWRC near saturation especially for $n < 2$ or $\alpha h_e > 1$ with unfavourable consequences for the performance of numerical models. Ippisch et al. (2006) introduced an air-entry value denoted by h_e in order to correct the unrealistic conductivity terms near saturation and proposed a modified van Genuchten-Mualem model,

$$S_e = \begin{cases} \frac{1}{S_c}[1 + (\alpha|h|)^n]^{-m}, & \text{for } h < h_e \\ 1, & \text{for } h \geqslant h_e \end{cases} \tag{8}$$

$$K(h) = \begin{cases} S_e^b \left[\frac{1 - \left(1 - (S_e S_c)^{1/m}\right)^m}{1 - \left(1 - S_c^{1/m}\right)^m}\right]^2 K_{sat}, & \text{for } h < h_e \\ K_{sat}, & \text{for } h \geqslant h_e, \end{cases} \tag{9}$$

where $S_c = [1 + (\alpha|h_e|)^n]^{-m}$ is the saturation degree at the cut-off point h_e in the classical van Genuchten model. For soils for which precisely measured unsaturated hydraulic conductivity data are not available, small values for the air-entry value h_e (e.g., -2 cm) are recommended by the authors.

2.4. Computation of the inter-nodal conductivity

The use of Equation (5) requires the computation of the average inter-cell conductivity $\overline{K}_{\alpha c}$. This is a non trivial subject and plays a crucial role in the

accuracy and convergence of the computational algorithm. Since, the hydraulic conductivity in unsaturated soils is a highly non linear function of the pressure head, the nodal conductivities can vary by several orders of magnitude. This makes the choice of the appropriate averaging procedure a difficult and case-dependent task. The most popular approach seems to be the standard arithmetic mean of nodal values, although it can produce significant errors in some flow situations (Baker, 2000; Belfort and Lehman, 2005). Various alternative methods were proposed including the geometric, upstream - weighted and integrated means.

Inter-comparisons of these approximations can be found in the literature (e.g Srivastava and Guzman-Guzman (1995); Belfort and Lehman (2005)) but the conclusions cannot be generalised because the numerical experiments were performed for a limited number of flow conditions, soil materials and grid sizes. It should be noted that even if a simple averaging scheme is used, such as the arithmetic mean, the error introduced can be significantly reduced by grid refinement in the zones where large pressure gradients are expected. In this case the problem is to know a priori the critical grid size for which the averaging scheme leads to acceptable results.

In our model, besides the aforementioned averaging schemes, we also incorporate the approach proposed by Szymkiewicz (2009), which is more advantageous for coarser grids. This method is based on the shape of the steady state distribution of the pressure head between the neighbouring cells and distinguishes between three major flow types: infiltration, drainage and capillary rise. For each flow type the inter-cell average conductivity is computed using a different averaging scheme. It is reported in the literature (Baker, 2000; Gastó et al., 2002) that this type of analysis yields the most accurate approximation of inter-cell conductivity.

In order to investigate the importance of the inter-nodal conductivity averaging scheme we ran the heterogeneous infiltration problem of Kirkland et al. (1992) (see section 3.2) using five different averaging schemes, namely an arithmetic mean, geometric mean, upstream-weighted mean and two numerical in-

tegrated means, one using the Simpson's three-point rule and one using the Gauss-Kronrod quadrature. It is obvious from Figure 4 that the choice of the inter-nodal conductivity averaging scheme can play a crucial role on the result of the simulations, especially when we have to deal with sharp infiltration front such as the one of the examined test cases.

2.5. Improving the performance and accuracy of the model

At the surface cells, especially in case of large evaporation or large precipitation on dry soil, an unrealistic hydraulic head buildup can occur. We embed into the model a routine that prevents this situation: if the hydraulic head in a surface cell exceeds an a-priori user-specified ponding elevation then a switch from the constant flux boundary condition to that of a constant head occurs. Also, if the total flux from a ponded cell into the domain exceeds the specified surface flux by more than one percent, the boundary condition is restored to that of a constant flux. Ponded cells are accounted for in the model flow budget as constant head cells.

As already mentioned above, the hydraulic properties in the unsaturated zone are highly non linear functions of the pressure head. Especially when we have to deal with initially dry soils, very small changes in the soil water content can result to changes of hydraulic properties by many orders of magnitude. An iterative process combined with an adaptive time-stepping technique improves the accuracy while keeping the algorithm efficient at the same time. The iteration process requires first, at time step $t + \Delta t$ and iteration level $m + 1$, to use the hydraulic properties $\overline{K}_{\alpha c}^{t+\Delta t,m}(h_c^{t+\Delta t,m})$ and $C_c^{t+\Delta t,m}(h_c^{t+\Delta t,m})$ computed from the previous iteration level and combining them with Equation (5) to compute an intermediate total head $H_c^{t+\Delta t,inter}$. The total head at the iteration level $m + 1$, at time step $t + \Delta t$ is then computed using the following under-relaxation technique

$$H_c^{t+\Delta t,m+1} = \frac{H_c^{t+\Delta t,inter} + H_c^{t+\Delta t,m}}{2}, \tag{10}$$

which improves the rate of convergence. The iteration process is continued until a predifined convergence criterion is satisfied in terms of a user-defined level of accuracy. The selection of an appropriate criterion is evidently important for the quick convergence and accuracy of the model. For our model we use the convergence criterion proposed by Huang et al. (1996), which is formulated as

$$C_c^{t+\Delta t,m}|H_c^{t+\Delta t,m+1} - H_c^{t+\Delta t,m}| = |\theta_c^{t+\Delta t,m+1} - \theta_c^{t+\Delta t,m}| \leq \epsilon_\theta, \qquad (11)$$

where the superscript m denote the iteration level and ϵ_θ is the accuracy level. Furthermore, the efficiency of the algorithm is increased by introducing an adaptive time-stepping technique (Thoms et al., 2006). The user inputs a minimum and a maximum value for the time step, a maximum allowed number of iterations, a time-step multiplier and a time-step reduction factor. The time step at one time level depends on the maximum number of iterations among the cellular space at the previous time level. If this number is bigger than the 65% of the user-defined maximum number of iterations then the time step is divided by the reduction factor in anticipation of convergence difficulties in the next time step. If it is less than 35% then the time step is multiplied by a multiplier to speed up the simulation. If the algorithm does not converge within a given time step, the time step is reduced by the reduction factor and the iterative computations are restarted with the reduced time step. If the adjusted time step is bigger than its maximum or smaller than its minimum value the time step is set accordingly to the maximum or minimum time value.

3. Results from the application to test case studies

The presented model was applied to various test cases available from the literature, in order to evaluate its performance. These include experimental data, analytical solutions and numerical experiments. The first two test cases included experimental data of infiltration and drainage in an homogeneous soil, the second test case included numerical experiments in an heterogeneous soil structure and the third test case consisted of a 3-D analytical solution for a

box-shaped soil sample with simple boundary conditions and soil constitutive properties.

We chose as indicator of the efficiency of the presented model the error in the mass balance computation. The mass balance ratio

$$MBR = \frac{\Delta V}{V_{in} - V_{out}} \tag{12}$$

was used to evaluate the precision in computing the mass conservation at each cell (Morton and Mayers, 1994). ΔV is the volume of water stored in a cell at time t and V_{in} and V_{out} are the volumes of water entering and outgoing of the element. If the mass is conserved perfectly then MBR should be equal to 1. When the ingoing and outgoing volumes are very small, Equation (12) can generate numerical overflow because of division by zero and therefore a modified MBR was used:

$$MBR_m = \frac{V_{t+\Delta t}}{V_t + V_{in} - V_{out}}. \tag{13}$$

where $V_{t+\Delta t}$ and V_t are the volumes of water stored in a cell at time $t + \Delta t$ and t respectively. The error in the mass balance computation is then given by

$$\epsilon = 1 - MBR_m \tag{14}$$

During our simulations the error from Equation (14) was computed at each cell and an average mass balance error is computed for each time step of the simulation.

3.1. Variably saturated transient infiltration and drainage study.

The first test case is based on the laboratory experiments performed by Vauclin et al. (1979) and aims at evaluating the ability of the model to simulate the transient position of the water table in a laboratory scale soil box. Experiments were run on a slab of soil 3.0 m long, 2.0 m high and 0.05 m thick (Figure 1b, Vauclin et al. (1979)) filled with a fine sandy soil and characterized by an initial water table located at 0.65 m from the bottom. A constant flux of $q = 3.55$ m/d was applied to the left 0.50 m of the soil surface of the slab for 8 hours,

whereas the remainder of the surface was kept covered to prevent losses due to evaporation. The initial total head of the cells was set to 0.65 m and the right boundary cells were kept at this initial water table position throughout the 8-hour simulation. The grid size was assumed to be $\Delta x = 0.1$ m, $\Delta y = 0.05$ m (Δx and Δy refer to the horizontal and vertical directions respectively). The hydraulic parameters used in the simulation are summarized in Table 2. As shown in Figure 5 the model can reproduce the observed water table dynamics well and the average mass balance errors are kept low as it is shown in Figure 7.

The second test case refers to a laboratory experiment performed by Vauclin et al. (1975), who examined transient drainage in a fine sandy soil through a seepage face within a rectangular slab of soil 3.0 m long by 2.0 m high by 0.05 m thick. This was initially kept at hydrostatic equilibrium with a head $H = 1.45$ m. The experiment measured changes of moisture content and pressure head when the constant head boundary imposed on the side of the soil slab instantaneously dropped to $H = 0.75$ m. The measurements describe the changes until the water table is in equilibrium with the boundary condition $H = 0.75$ m. The right boundary above the water table was set as a seepage face. We used the same parameters and the same domain discretization of the first test case to simulate the first 5 hours of the experiment were simulated. The position of the water table shown in Figure 6 shows the drop of the water table over the first 5 of the 20 hours simulated experiment and indicates that the model is capturing extremely well over the entire range of distances the experimental data. Mass balance errors are, as a consequence, also kept low, as it is shown in Figure 7.

For these two test cases we also conducted numerical simulations using VSF-MODFLOW (Thoms et al., 2006), in order to assess the performance of our algorithm compared to a state-of-the art numerical code in terms of accuracy and computational efficiency. VSF-MODFLOW is an extension to the popular 3-D finite difference groundwater model MODFLOW (Harbaugh et al., 2000) and it is based on the implicit discretization of the Richards' equation using the modified Picard iteration technique (Celia et al., 1990). All the model

runs were done on a MacBook Pro with an Intel Core 2 Duo Processor at 3.06 GHz and 8 GB of RAM memory. The simulation of the infiltration experiment took 6.19 seconds and 7.57 seconds using our computational scheme and VSF-MODFLOW respectively (18.23% faster), while the time for the drainage experiment was 10.25 seconds and 11.87 seconds respectively (13.65% faster). The gain in computational time is sizeable even for these very small scale studies, especially taking into account that our code is totally unoptimized, while VSF-MODFLOW has been developed for many years. The results make us confident that the performance gain will be even more notable with larger scale problems, for which our approach scales almost linearly with the spatial scale of the problem due to its explicit nature, in contrast to VSF-MODFLOW, which solves iteratively a non-linear system. The average time step and number of iterations for the infiltration experiment, finally, were 29.91 seconds and 9.46 iterations respectively, while for the drainage experiment 23.81 seconds and 11.48 iterations respectively. In terms of accuracy, as it is shown in Figures 5 and 6, both models produce consistently good results.

3.2. Flow in heterogeneous soil.

In order to test the performance of our model in a case similar to the prospective application of this model we used two numerical experiments proposed by Kirkland et al. (1992). They designed test problems to show the performance of the algorithms in two dimensions for both very dry and variably saturated conditions in heterogeneous soils. In particular, these tests represent a challenge for numerical algorithms due to their strongly non linear nature. The hydraulic parameters used in these simulations are shown in Table 3 and the grid size for both numerical experiments is $\Delta x = \Delta y = 0.5$ cm.

The first test case is a challenging two-dimensional infiltration problem involving strictly unsaturated conditions. It consists of simulating the flow within a region 5.0 m wide by 3.0 m deep, which is divided into nine alternating blocks of clay and sand, as illustrated by Figure 8. A constant flux of 0.05 m/d is applied over a 1 m width at the center of the top boundary with zero flux

boundary conditions elsewhere. The simulation was run with initial pressure head all over the computational domain of -500 m, to mimic a very dry initial condition. We examined the pressure distribution after 12.5 days of constant load and we could observe, as shown in Figure 9, that our simulation compares very well with the reference numerical solution by Kirkland et al. (1992).

The second test problem models the development of a perched water table surrounded by very dry unsaturated conditions. This problem aims at testing the ability of numerical algorithms to cope both with very dry conditions and with transition to saturated conditions. The computational domain consists of a symmetric region of 5.0 m by 3.0 m. In order to achieve a perched water table a 3.0 m by 1.0 m region of sand was bounded by a 1.0 m clay domain on both sides and underneath, below which in turn a 1.0 m layer of sand was placed (see Figure 10). The initial pressure head was also in this case -500 m all over the computational domain to achieve a very dry soil initial condition. Similarly to the first test problem a flux of 0.5 m/d was imposed on the sand and we examined the pressure distribution after 1 day of constant load. The result of the simulation, compared with the numerical solution by Kirkland et al. (1992) in Figure 11, shows that our model is capable of reproducing very well the reference contour pressures over the entire domain. Figure 12 confirms this by showing how the average mass balance error is negligible for both flow test cases.

3.3. 3-D unsaturated flow in a box-shaped soil sample.

In this test case we finally validated the ability of the algorithm to successfully simulate 3-D flow conditions. The problem consists of modelling the flow through a very dry prismatic block of soil having dimensions $a \times b \times L$ along a cartesian reference system x, y, z, where a and b are the horizontal dimensions and L is the vertical one. The analytical solution, which provides the pressure head distribution following the infiltration and which we use as benchmark for our simulation, follows the solution of Richards' equation obtained using a method that transforms the equation into a linear partial differential equation

(Tracy, 2006). The hydraulic functions used for the derivation of this analytical solution are defined by the following equations

$$\begin{aligned} \theta &= \theta_r + (\theta_s - \theta_r)e^{\alpha h} \\ K(h) &= e^{\alpha h} k_s \end{aligned} \tag{15}$$

The test problem we ran to validate our simulation is the same as the run by Tracy (2006). Water is applied to the domain specified at $z = L$ such that the pressure head, h, is zero at the center of the domain and decreases towards the outer edges where it is equal to the dry soil pressure head h_r. The latter condition is also given on all of the other boundaries except for $z = L$, where it is defined by the equation

$$h(x, y, L, t) = \frac{1}{\alpha} \ln\big(e^{\alpha h_r} + (1 - e^{\alpha h_r}) \sin \frac{\pi x}{a} sin \frac{\pi y}{b}\big), \tag{16}$$

where α is a parameter. The solution to compute analytically the pressure head h at the generic position x, y, z and at time t is provided by Tracy's equation (46) (Tracy, 2006):

$$\begin{aligned} h(x, y, z, t) = \frac{1}{\alpha} \ln \Bigg\{ & e^{\alpha h_r} + h_0 sin \frac{\pi x}{a} sin \frac{\pi y}{b} e^{\alpha/2(L-z)} \\ & \left[\frac{\sinh \beta z}{\sinh \beta L} + \frac{2}{Lc} \sum_{q=1}^{\infty} (-1)^q \frac{\lambda_q}{\gamma} sin(\lambda_q z) e^{-\gamma t} \right] \Bigg\}, \end{aligned} \tag{17}$$

where $c = \frac{\alpha(\theta_s - \theta_r)}{k_s}$, $\gamma = \frac{1}{c}(\beta^2 + \lambda_q^2)$, $\beta = \sqrt{\frac{\alpha^2}{4} + \left(\frac{\pi}{a}\right)^2 + \left(\frac{\pi}{b}\right)^2}$, $h_0 = 1 - e^{\alpha h_r}$, $\lambda_q = \frac{q\pi}{L}$, k_s is the saturated hydraulic conductivity, α is an empirical parameter and θ_s and θ_r are respectively the saturated and the residual soil moisture.

The model domain that is selected for the needs of this validation test is a homogeneous soil cube of size $a = b = L = 10$ m, which is divided in a uniform grid of $\Delta x = \Delta y = \Delta z = 0.25$ m. Consistently with the test problem simulated by Tracy, the soil parameters used are: $\theta_s = 0.45$, $\theta_r = 0.15$, $k_s = 10^{-5}$ m/s and $h_r = -10$ m. The value of parameter α is crucial because it affects the shape of the soil water retention curve and thus the non-linearity of the problem, in turn causing difficulties in the convergence of the algorithm and a growth of the computational error. We ran our simulations for three different values of the

parameter α, i.e. 0.164 1/m, 0.328 1/m and 0.492 1/m , which were also used by Tracy (2006).

During each time step of the simulation the pressure head and its deviation from the analytical solution were computed at every cell of the domain. Figure 13 shows the distribution of pressure head versus depth plotted for three different points of the domain and for different values of the paramerer α. Figure 14 shows the distribution of the maximum percentage error during the simulations. The mode of the distribution of the maximum percentage error is always lower than 0.5%, thus showing that even if the computational error increases with increasing α, the agreement of our simulated values with Tracy's analytical solution is very good. This result is further demonstrated in Figure 15, where the distribution of the average mass balance error is shown to peak around values between 10^{-6} and 10^{-8} depending on the value of the parameter α. Figure 16 shows, finally, the plot of the average mean error and the root mean square error (RMSE) of the pressure head for the computational domain and for all the simulation time. Deviations from the analytical solution start developing at the beginning of the simulation when the soil conditions are very dry and strong non-linearities exist. The deviations keep growing during the transient phace of the simulation and they tend to stabilize as we reach the steady-state phace of the simulation.

4. Summary, conclusions and future perspectives

The use of the cellular automata framework is widespread in various disciplines for the modelling of complex system procedures. In this paper, it is used for the development of a reduced complexity model for the simulation of variably saturated flow in soils. The inherent CA concept simplicity and its natural parallelism make it a very efficient tool for the simulation of large scale phenomena.

It is shown in the Appendix A of Mendicino et al. (2006) that the derivation of the proposed computational scheme is a special case of a more general direct discrete formulation of the unsaturated flow problem. Following this

approach the discrete-to-continuum-to-discrete paradox (Toffoli, 1984; Tonti, 2001) is avoided and the problem is described in a more straight-forward way. When a rectangular spatial grid discretization is used, this formulation is similar to finite differences (FD) or finite volumes method schemes (FVM). But if an irregular grid is used there is a potential for modelling flow problems using a simple FD-like computational kernel based on a cell assembly similar to Finite Elements Method (FEM) analysis. This approach, combined with a parabolic interpolation function for each cell, is reported to have a higher order of convergence compared to the one obtained with the FEM using the same interpolation function (Tonti, 2001). The most notable advantage of this approach is its massive parallel nature which leads to a computational cost of the method that is linear with respect to the number of the cells, thus making it very attractive for parallel computing.

In the present days, due to the considerable hardware advancements even at the level of desktop computers, parallel computing becoming an increasingly available resource, which does not require necessarily only expensive clusters. Most of the consumer desktop computers have quad-core or even six-core processors and powerful multi-core graphics cards, thus making the design and execution of parallel code easier than ever before. We are currently planning the development of parallel versions of our computational framework utilizing the OpenMP$_{\mathrm{TM}}$[1] and CUDA$_{\mathrm{TM}}$[2] prototypes, to prepare the application to the simulation of complex slope stability problems at the catchment scale. OpenMP$_{\mathrm{TM}}$ follows the shared memory architecture and with minimal changes it can turn a sequential algorithm into a parallel one, which can take advantage of the multi-core processor personal computers. CUDA$_{\mathrm{TM}}$ prototype is used to execute an algorithm over the numerous streaming multiprocessors of

[1] OpenMP is a multi-platform, shared-memory Application Program Interface (API), which gives programmers a simple and flexible interface for developing parallel applications for platforms ranging from the desktop to the supercomputer.

[2] CUDA is NVIDIA's parallel computing architecture. It enables dramatic increases in computing performance by harnessing the power of the GPU.

an NVIDIA$_{\mathrm{TM}}$ graphics card. Depending on the used graphic card, the gain in performance can be substantial.

The robustness and the efficiency of the proposed model, demonstrated through simple but challenging simulations of several test case studies, suggest that the CA framework jointly with appropriate software and hardware technology can lead to significant progress in modelling physically consistent formulations of complex hydrological problems. The proposed model can be easily incorporated into a more general catchment scale distributed hydrological model for the simulation of the water balance or in other types of models, which need to simulate the dynamics of water pressure heads and of soil saturation, such as the simulation of rainfall triggered landslides and of solute and contaminant transport in agricultural soils, to name a few of particular interest. In all these cases the complexity of the required models poses a serious constraint to their predictive use, especially in the real time context. The increased efficiency due to a reduced computation time, jointly with the easy parallelisation of the code, can be an important asset to improve the reliability of the prediction of complex natural hazard phenomena.

Acknowledgements

This study was developed within the context of the EU FP7 project ACQWA (Assessing Climatic change and impacts on the Quantity and quality of Water), Grant agreement no. 212250. We greatly appreciate the comments of two anonymous reviewers and of Prof. S. Elmaloglou that contributed to improve the quality of the manuscript.

Appendix: Convergence analysis of the proposed method

The most basic property of a numerical scheme, in order to be successful, is that its solutions approximate the exact solution and that the approximation improves as the computational grid spacings tend to zero. Hence, a numerical scheme is convergent at point (x, y, z, t) if the numerical solution $\hat{H}(x, y, z, t)$

converges to the exact solution $H(x,y,z,t)$ as $(i\cdot\Delta x, j\cdot\Delta y, k\cdot\Delta z, t\cdot\Delta t)$ tends to (x,y,z,t) while $\Delta x, \Delta y, \Delta z, \Delta t \to 0$. Introducing the error ϵ as

$$\epsilon^t_{i,j,k} = H^t_{i,j,k} - \hat{H}^t_{i,j,k} \tag{A.1}$$

that is the difference between the exact solution H and the discrete solution $\hat{H}$ at the grid point (i,j,k,t).

The approximate solution can be written as $\hat{H}^t_{i,j,k} = H^t_{i,j,k} - \epsilon^t_{i,j,k}$ according to Equation (A.1). Substituting this expression in Equation (2) and considering a uniform grid ($\Delta x = \Delta y = \Delta z = l$, $A_{ca} = l^2$, $V_c = l^3$) we get the following relationship for the introduced error term for the generic point $(i,j,k,t+\Delta t)$

$$\begin{aligned}
\epsilon^{t+\Delta t}_{i,j,k} &= \frac{1}{1+\Gamma}\epsilon^t_{i,j,k} + \frac{\Delta t}{\sigma^t_{i,j,k} l^2(1+\Gamma)} \cdot \\
&\cdot \Big(\overline{K}^t_{i-1,j,k}\epsilon^t_{i-1,j,k} + \overline{K}^t_{i+1,j,k}\epsilon^t_{i+1,j,k} + \overline{K}^t_{i,j-1,k}\epsilon^t_{i,j-1,k} \\
&+ \overline{K}^t_{i,j+1,k}\epsilon^t_{i,j+1,k} + \overline{K}^t_{i,j,k-1}\epsilon^t_{i,j,k-1} + \overline{K}^t_{i,j,k+1}\epsilon^t_{i,j,k+1}\Big) \\
&- \frac{1}{\sigma^t_{i,j,k} l^3(1+\Gamma)} S_c + L(H,K)
\end{aligned} \tag{A.2}$$

where $\overline{K}^t_{sum} = \Big(\overline{K}^t_{i-1,j,k} + \overline{K}^t_{i+1,j,k} + \overline{K}^t_{i,j-1,k} + \overline{K}^t_{i,j+1,k} + \overline{K}^t_{i,j,k-1} + \overline{K}^t_{i,j,k+1}\Big)$, $\Gamma = \frac{\Delta t}{\sigma^t_{i,j,k} l^2}\overline{K}^t_{sum}$, $\sigma^t_{i,j,k} = \sigma(h_c)$, h_c is the pressure head and $L(H,K)$ is a function of the permeability and the exact solution

$$\begin{aligned}
L(H,K) &= H^{t+\Delta t}_{i,j,k} - \frac{1}{1+\Gamma}H^t_{i,j,k} - \frac{\Delta t}{\sigma^t_{i,j,k} l^2(1+\Gamma)} \cdot \\
&\cdot \Big(\overline{K}^t_{i-1,j,k}H^t_{i-1,j,k} + \overline{K}^t_{i+1,j,k}H^t_{i+1,j,k} + \overline{K}^t_{i,j-1,k}H^t_{i,j-1,k} \\
&+ \overline{K}^t_{i,j+1,k}H^t_{i,j+1,k} + \overline{K}^t_{i,j,k-1}H^t_{i,j,k-1} + \overline{K}^t_{i,j,k+1}H^t_{i,j,k+1}\Big)
\end{aligned} \tag{A.3}$$

To keep things simple we will not consider the source term S_c. Let M be the maximum modulus of $L(H,K)$ for all (i,j,k,t) ($|L(H,K)| \leq M$). Equation (A.2) can be rewritten as

$$|e^{t+\Delta t}_{i,j,k}| \leq \frac{1}{1+\Gamma}|e^{t}_{i,j,k}| + \frac{\beta_{i-1,j,k}}{1+\Gamma}|e^{t}_{i-1,j,k}| + \cdots + \frac{\beta_{i,j,k+1}}{1+\Gamma}|e^{t}_{i,j,k+1}| + M \tag{A.4}$$

where $\beta_{i-1,j,k} = \frac{\Delta t}{\sigma^t_{i,j,k} l^2}\overline{K}^t_{i-1,j,k}$, ... , $\beta_{i,j,k+1} = \frac{\Delta t}{\sigma^t_{i,j,k} l^2}\overline{K}^t_{i,j,k+1}$.

In the above equation it holds $0 \leq \frac{1}{1+\Gamma} \leq 1$ and for the coefficients of the errors at the neighbouring cells we have: $\beta_{i-1,j,k} < \Gamma$ because $\overline{K}^t_{i-1,j,k} < \overline{K}^t_{sum}$ and $\frac{\beta i-1,j,k}{1+\Gamma} < \frac{\beta_{i-1,j,k}}{\Gamma} < 1$ so that the previous inequality takes the following form:

$$|\epsilon^{t+\Delta t}_{i,j,k}| \leq |\epsilon^{t}_{i,j,k}| + |\epsilon^{t}_{i-1,j,k}| + \cdots + |\epsilon^{t}_{i,j,k+1}| + M \tag{A.5}$$

Let's denote $E^t_{max} = \max|\epsilon^t_{i,j,k}|$ and $E^{t+\Delta t}_{max} = \max|\epsilon^{t+\Delta t}_{i,j,k}|$. The previous inequality holds for all values of $|\epsilon^{t+\Delta t}_{i,j,k}|$ and $|\epsilon^{t}_{i,j,k}|$ so it holds also for $E^{t+\Delta t}_{max}$ and E^t_{max}. Working by induction, the previous equation can be written as

$$E^{t+\Delta t}_{max} \leq 6 \cdot E^t_{sum} + M \leq 6 \cdot (6 \cdot E^{t-\Delta t}_{sum} + M) + M = 6^2 \cdot E^{t-\Delta t}_{sum} + (6+1)M, \tag{A.6}$$

etc., from which it follows that

$$E^{t+\Delta t}_{max} \leq 6^n \cdot E^0_{max} + (1 + 6 + \cdots + 6^n) \cdot M = (1 + 6 + \cdots + 6^n) \cdot M \tag{A.7}$$

where $E^0_{max} = 0$ because the initial values for $\hat{H}$ and H are the same. Rearranging Equation (A.3)

$$\begin{aligned} L(H,K) &= \frac{\Delta t}{\sigma^t_{i,j,k} l^2 (1+\Gamma)} \Bigg[\sigma^t_{i,j,k} V_c \frac{H^{t+\Delta t}_{i,j,k} - H^t_{i,j,k}}{\Delta t} - \frac{A_{c\alpha}}{l_{c\alpha}} \cdot \\ &\cdot \Big(\overline{K}^t_{i-1,j,k} H^t_{i1,j,k} + \overline{K}^t_{i+1,j,k} H^t_{i+1,j,k} + \overline{K}^t_{i,j-1,k} H^t_{i,j-1,k} \\ &+ \overline{K}^t_{i,j+1,k} H^t_{i,j+1,k} + \overline{K}^t_{i,j,k-1} H^t_{i,j,k-1} + \overline{K}^t_{i,j,k+1} H^t_{i,j,k+1} \\ &- \overline{K}^t_{sum} H^{t+\Delta t}_{i,j,k} \Big) \Bigg] \end{aligned} \tag{A.8}$$

it can be observed that as $\Delta x, \Delta y, \Delta z, \Delta t \rightarrow 0$ the term in brackets tends to the differential form of the mass balance equation for the generic cell of the computational grid. Hence $L(H, K) \rightarrow 0 \Leftrightarrow M \rightarrow 0$ and from Equation (A.7) $|\epsilon_{i,j,k}^{t+\Delta t}| \leq E_{max}^{t+\Delta t} \leq 0 \Leftrightarrow |\epsilon_{i,j,k}^{t+\Delta t}| = 0$ when $\Delta x, \Delta y, \Delta z, \Delta t \rightarrow 0$, which proves that the numerical solution $\hat{H}$ converges to the exact solution H and the time-step Δt which is chosen for the simulation is independent of the cell size $\Delta x, \Delta y, \Delta z$ and the cell's hydraulic properties.

References

Baker, D., 2000. A Darcian integral approximation to interblock hydraulic conductivity means in vertical infiltration. Computers & Geosciences 26, 581–590.

Barpi, F., Borri-Brunetto, M., Veneri, L. D., 2007. Cellular-Automata Model for Dense-Snow Avalanches. Journal of Cold Regions Engineering 21, 121–140.

Belfort, B., Lehman, F., 2005. Comparison of Equivalent Conductivities for Numerical Simulation of One-Dimensional Unsaturated Flow. Vadose Zone Journal 4, 1191–1200.

Brooks, R., Corey, T., 1964. Hydraulic properties of porous media. Hydrol. Pap. 3, Colo. State Univ., Fort Collins.

Celia, M. A., Bouloutas, E. T., D., Zarba, R. L., 1990. A general mass-conservative numerical solution for the unsaturated flow equation. Water Resources Research 26, 1483–1496.

Chau, J. F., Or, D., Sukop, M. C., 2005. Simulation of gaseous diffusion in partially saturated porous media under variable gravity with lattice Boltzmann methods. Water Resources Research 41, 1–11.

Chen, H., Chen, S., Matthaeus, W., 1992. Recovery of the Navier-Stokes equations using a lattice-gas Boltzmann method. Physical Review A 45, 5339–5342.

Clement, T., Wise, W., Molz, F., 1994. A physically based, two-dimensional, finite-difference algorithm for modeling variably saturated flow. Journal of Hydrology 161, 71–90.

D' Ambrosio, D., Iovine, G., Spataro, W., Miyamoto, H., 2007. A macroscopic collisional model for debris-flows simulation. Environmental Modelling & Software 22, 1417–1436.

Fahs, M., Younes, A., Lehmann, F., 2009. An easy and efficient combination of the Mixed Finite Element Method and the Method of Lines for the resolution of Richards Equation. Environmental Modelling & Software 24, 1122–1126.

Frisch, U., D' Humieres, D., Hasslacher, B., Lallemand, P., Pomeau, Y., Rivet, J., 1987. Lattice gas hydrodynamics in two and three dimensions. Complex Systems 1, 649–707.

Gastó, J. M., Grifoll, J., Cohen, Y., 2002. Estimation of internodal permeabilities for numerical simulation of unsaturated flows. Water Resources Research 38, 1–10.

Harbaugh, A. W., Banta, E. R., Hill, M., McDonald, M. G., 2000. MODFLOW2000, the U.S. Geological Survey modular groundwater modeluser guide to modularization concepts and the Groundwater Flow Process. U.S. Geological Survey Open-File Report 0092.

Huang, K., Mohanty, B. P., van Genuchten, M., 1996. A new convergence criterion for the modified Picard iteration method to solve the variably saturated flow equation. Journal of Hydrology 178, 69–91.

Ippisch, O., Vogel, H.-J., Bastian, P., 2006. Validity limits for the van Genuchten–Mualem model and implications for parameter estimation and numerical simulation. Advances in Water Resources 29, 1780–1789.

Kirkland, M., Hills, R., Wierenga, P., 1992. Algorithms for Solving Richards Equation for Variably Saturated Soils. Water Resources Research 28, 2049–2058.

Manzini, G., Ferraris, S., 2004. Mass-conservative finite volume methods on 2-D unstructured grids for the Richards equation. Advances in Water Resources 27, 1199–1215.

McBride, D., Cross, M., Croft, N., Bennett, C., Gebhardt, J., 2006. Computational modelling of variably saturated flow in porous media with complex three-dimensional geometries. International Journal for Numerical Methods in Fluids 50, 1085–1117.

McNamara, G., Zanetti, G., 1988. Use of the Boltzmann equation to simulate lattice gas automata. Physical review letters 61, 2332–2335.

Mendicino, G., Senatore, A., Spezzano, G., Straface, S., 2006. Three-dimensional unsaturated flow modeling using cellular automata. Water Resources Research 42.

Morton, K., Mayers, D., 1994. Numerical solution of partial differential equations. Cambridge University Press.

Qian, Y. H., D'Humières, D., Lallemand, P., 1992. Lattice BGK Models for Navier-Stokes Equation. Europhysics Letters 17, 479–484.

Ravazzani, G., Rametta, D., Mancini, M., 2011. Macroscopic cellular automata for groundwater modelling: A first approach. Environmental Modelling & Software 26, 634–643.

Richards, L., 1931. Capillary conduction of liquids through porous mediums. Physics 1, 318–333.

Rongo, R., Spataro, W., D' Ambrosio, D., Vittoria, M., 2008. Lava Flow Hazard Evaluation Through Cellular Automata and Genetic Algorithms : an Application to Mt Etna Volcano. Fundamenta Informatica 87, 247–267.

Sadegh Zadeh, K., 2011. A mass-conservative switching algorithm for modeling fluid flow in variably saturated porous media. Journal of Computational Physics 230, 664–679.

Schaap, M. G., van Genuchten, M. T., 2005. A Modified Mualem-van Genuchten Formulation for Improved Description of the Hydraulic Conductivity Near Saturation. Vadose Zone Journal 5, 27–34.

Seybold, H. J., Molnar, P., Singer, H. M., Andrade, J. S., Herrmann, H. J., Kinzelbach, W., 2009. Simulation of birdfoot delta formation with application to the Mississippi Delta. Journal of Geophysical Research 114, 1–13.

Srivastava, R., Guzman-Guzman, A., 1995. Analysis of Hydraulic Conductivity Averaging Schemes for One-Dimensional, Steady-State Unsaturated Flow. Ground Water 33, 946–952.

Succi, S., Benzi, R., Higuera, F., 1991. The lattice Boltzmann equation: A new tool for computational fluid dynamics. Physica D 47, 219–230.

Sukop, M. C., Or, D., 2004. Lattice Boltzmann method for modeling liquid-vapor interface configurations in porous media. Water Resources Research 40, 1–11.

Szymkiewicz, A., 2009. Approximation of internodal conductivities in numerical simulation of one-dimensional infiltration, drainage, and capillary rise in unsaturated soils. Water Resources Research 45, 1–16.

Thoms, R., Johnson, R. L., Healy, R. W., 2006. Users Guide to the Variably Saturated Flow (VSF) Process for MODFLOW. U.S. Geological Survey Techniques and Methods, Reston, Virginia.

Toffoli, T., 1984. Cellular Automata as an Alternative to (rather than an approximation of) Differential equations in modeling physics. Physica 10D, 117–127.

Tonti, E., 2001. A direct discrete formulation of field laws: The cell method. Computer Modeling in Engineering & Sciences 2, 237–258.

Tracy, F. T., 2006. Clean two- and three-dimensional analytical solutions of Richards' equation for testing numerical solvers. Water Resources Research 42, 1–11.

van Dam, J. C., Feddes, R. A., 2000. Numerical simulation of infiltration, evaporation and shallow groundwater levels with the Richards equation. Journal of Hydrology 233, 72–85.

van Genuchten, M. T., Nielsen, D. R., 1985. On describing and predicting the hydraulic properties of unsaturated soils. Annales Geophysicae 3, 615–628.

Vauclin, M., Khanji, D., Vachaud, G., 1979. Experimental and numerical study of a transient, two-dimensional unsaturated-saturated water recharge problem. Water Resources Research 15, 1089–1101.

Vauclin, M., Vachaud, G., Khanji, J., 1975. Two dimensional numerical analysis of transient water transfer in saturated-unsaturated soils. Modeling and Simulation of Water Resources Systems, North-holland, Amsterdam, 299–323.

Vogel, T., van Genuchten, M. T., Cislerova, M., 2001. Effect of the shape of the soil hydraulic functions near saturation on variably-saturated flow predictions. Advances in Water Resources 24, 133–144.

von Neumann, J., 1966. Theory of Self-Reproducing Automata. University of Illinois Press.

Šimůnek, J., van Genuchten, M. T., Šejna, M., 2008. Development and Applications of the HYDRUS and STANMOD Software Packages and Related Codes. Vadose Zone Journal 7, 587.

Williams, G., Miller, C., Kelley, C., 2000. Transformation approaches for simulating flow in variably saturated porous media. Water Resources Research 36, 923–934.

Wolfram, S., 1986. Theory and Application of Cellular Automata. World Scientific.

Wolfram, S., 1994. Cellular Automata and Complexity. Addison-Wesley.

Zhang, X. X., Deeks, L. K., Bengough, A. G., Crawford, J. W., Young, I. M., 2005. Determination of soil hydraulic conductivity with the lattice Boltzmann method and soil thin-section technique. Journal of Hydrology 306, 59–70.

List of Figures

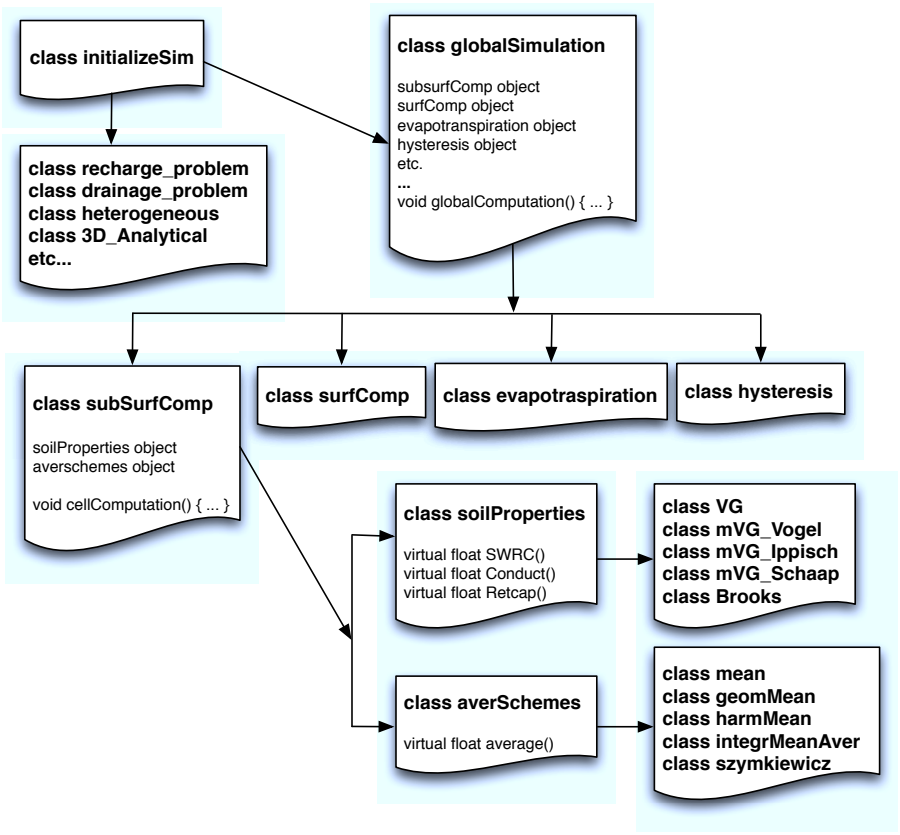

Figure 1: Flowchart of the computational framework

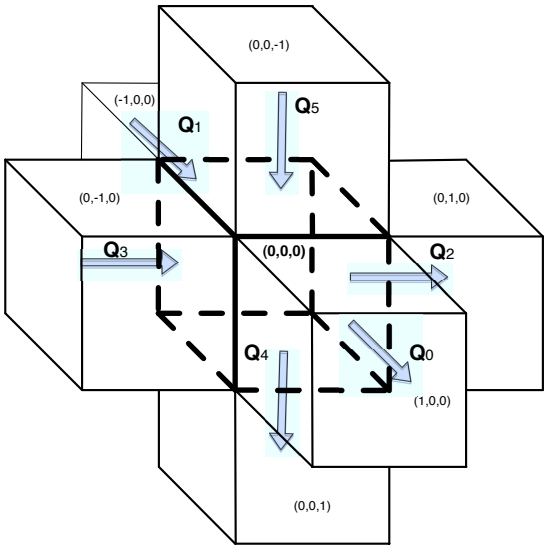

Figure 2: Neighborhood of a generic cell for a CA framework

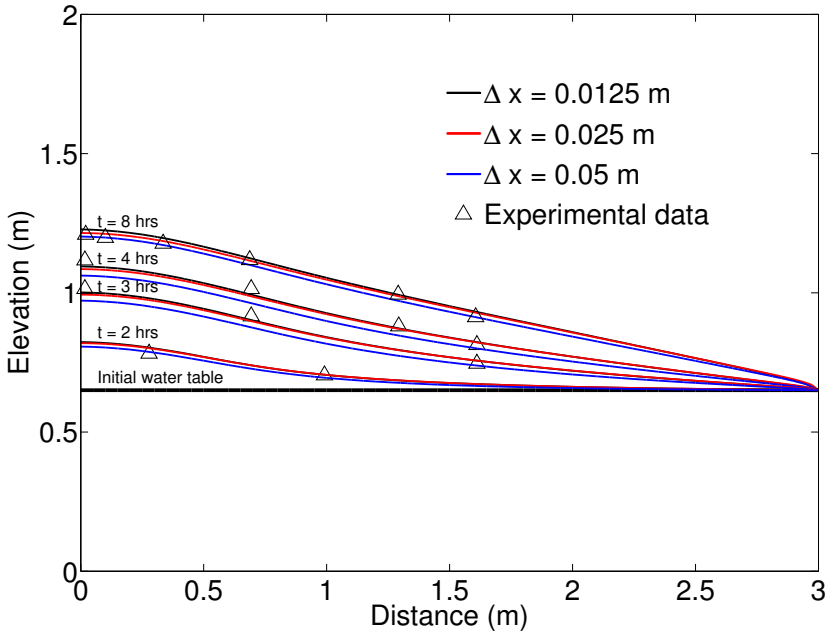

Figure 3: Convergence analysis of the algorithm for the infiltration experiment of Vauclin et al. (1979) using three different spatial grids

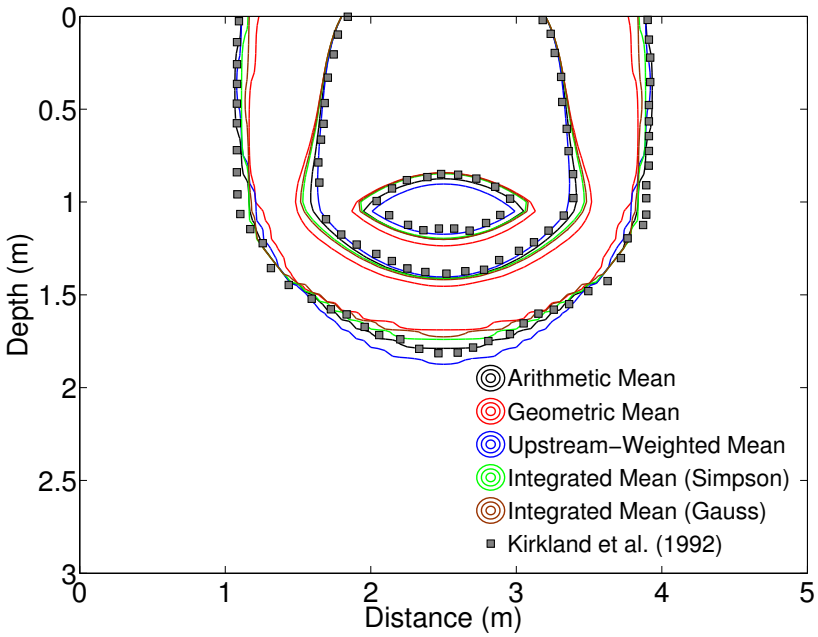

Figure 4: Comparison of different inter-nodal conductivity averaging schemes for the heterogeneous infiltration numerical experiment of Kirkland et al. (1992)

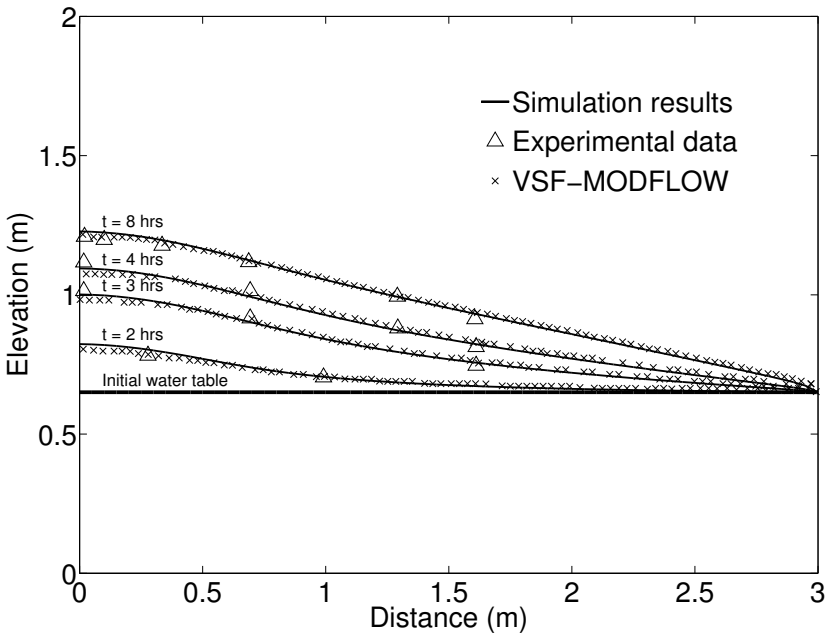

Figure 5: Simulated vs observed water table rise for the two dimensional variably saturated transient infiltration test case by Vauclin et al. (1979)

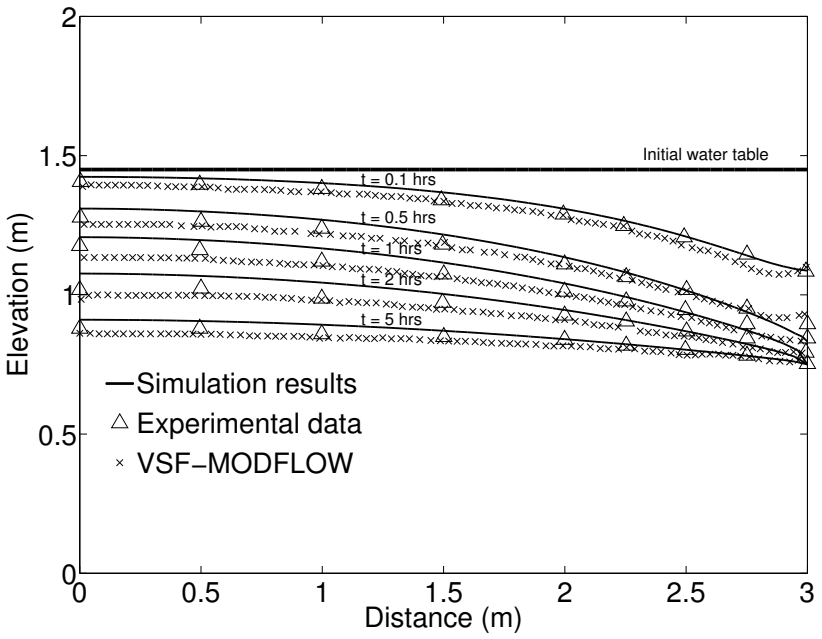

Figure 6: Simulated vs observed water table decline for the two dimensional variably saturated transient drainage test case by Vauclin et al. (1975).

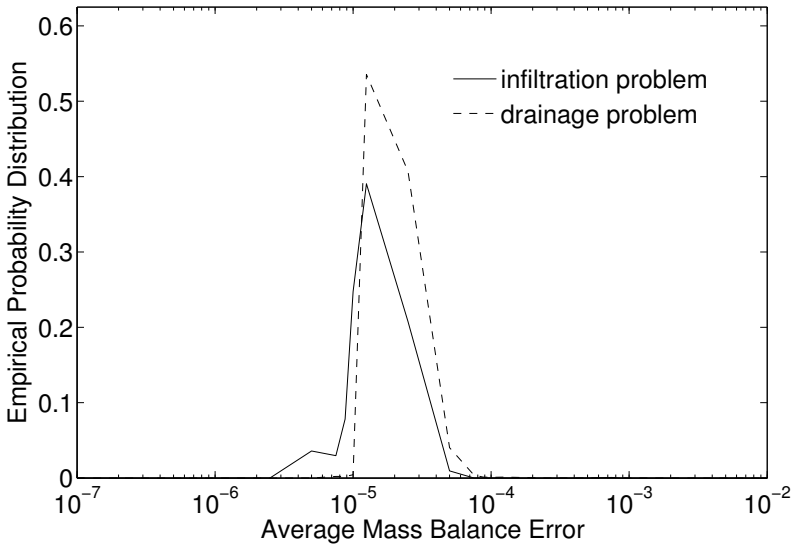

Figure 7: Empirical probability distribution of the average mass balance error for the infiltration (Vauclin et al., 1979) and drainage (Vauclin et al., 1975) test cases.

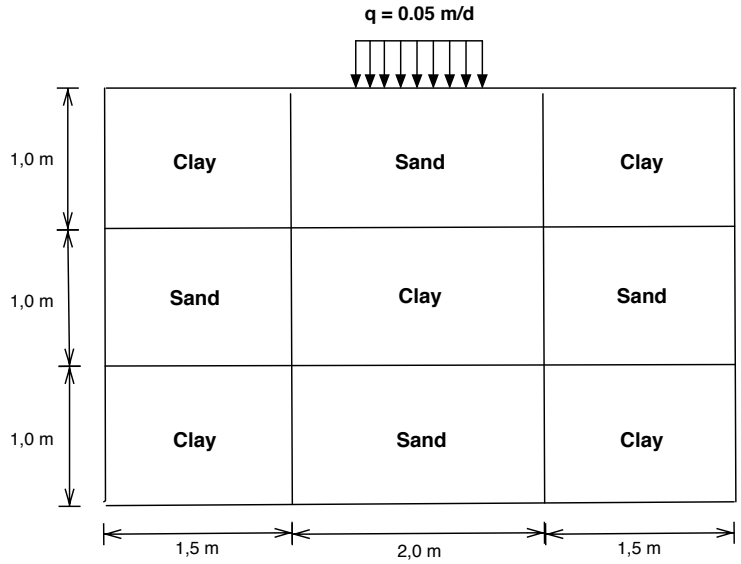

Figure 8: Domain layout for the simulation of the first test case of flow in heterogeneous soil by Kirkland et al. (1992).

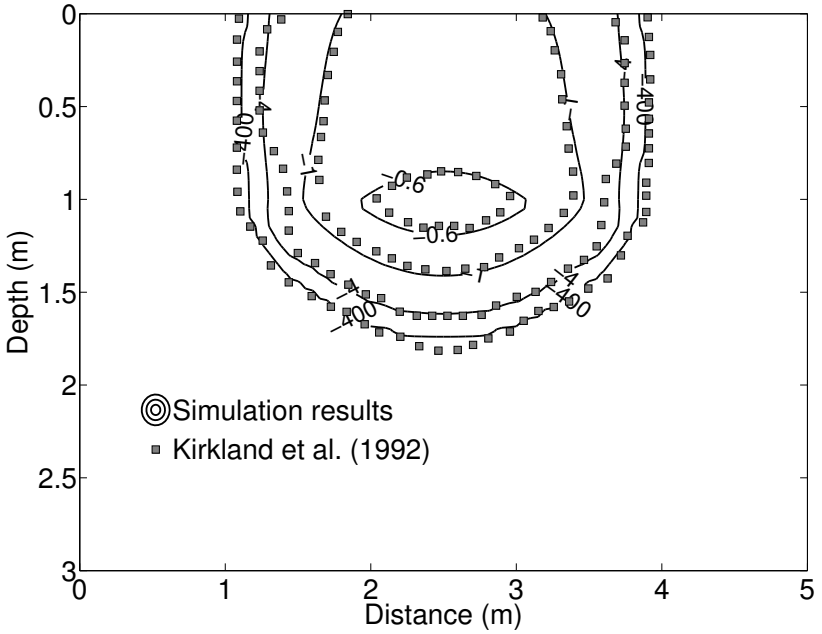

Figure 9: Comparison of model simulation with the reference numerical solution by Kirkland et al. (1992) for the first of the test cases of flow in heterogeneous soils. The simulated contour pressure [m] are shown after 12.5 days of constant load.

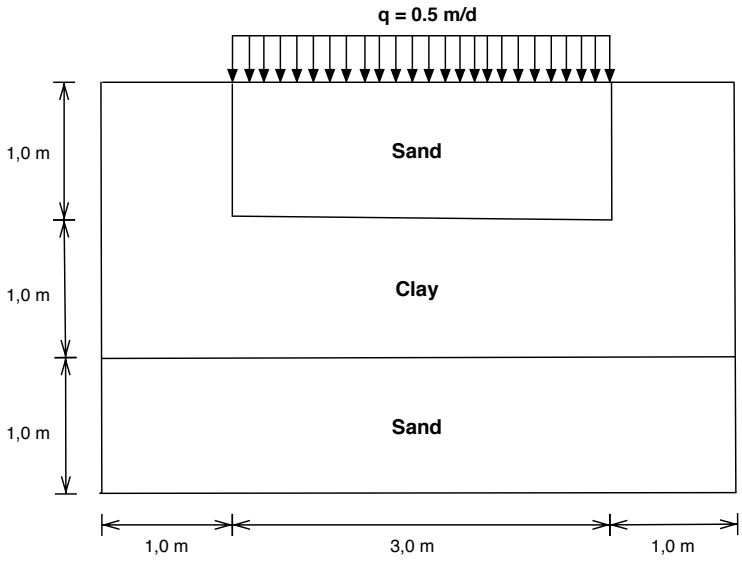

Figure 10: Domain layout for the simulation of the second test case of flow in heterogeneous soil (perched water table) by Kirkland et al. (1992).

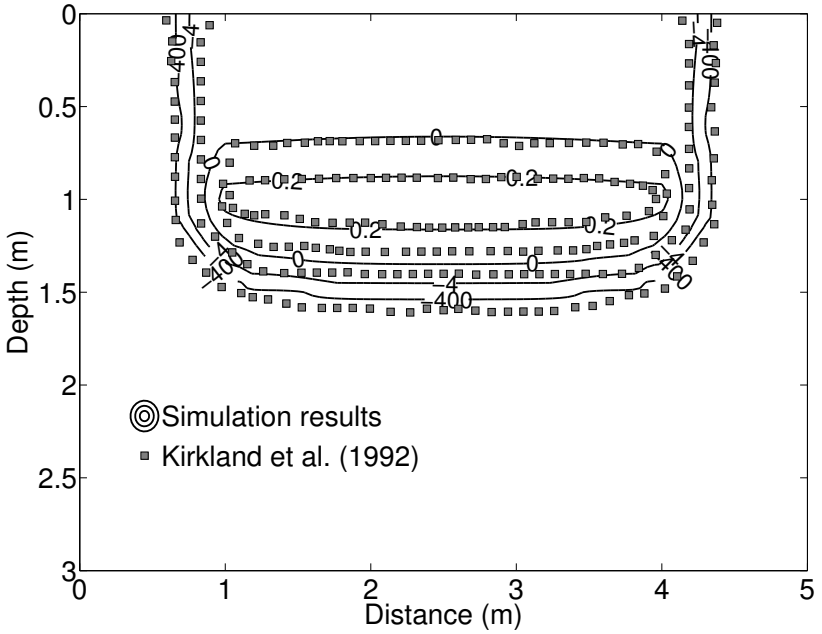

Figure 11: Comparison of model simulation with the reference numerical solution by Kirkland et al. (1992) for the second of the test cases of flow in heterogeneous soils. The simulated contour pressure [m] are shown after 1 day of constant load.

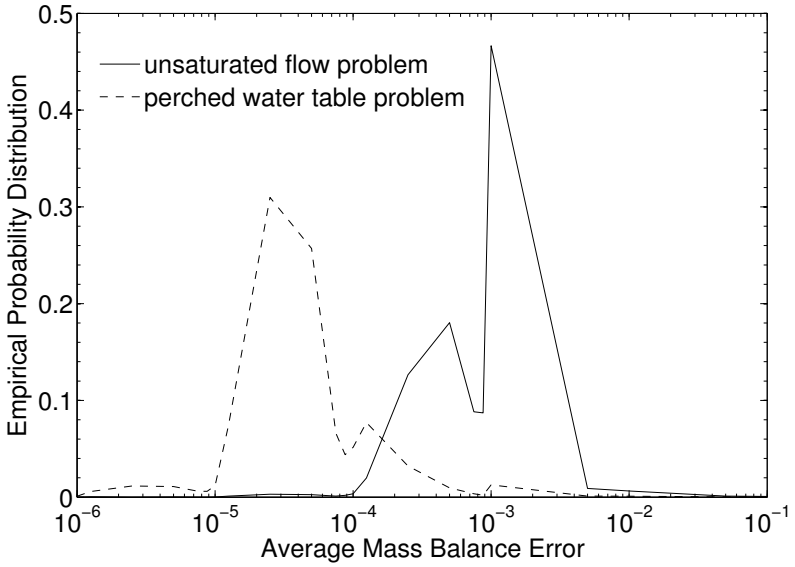

Figure 12: Empirical probability distribution of the average mass balance error for the two heterogeneous soil flow test cases by Kirkland et al. (1992).

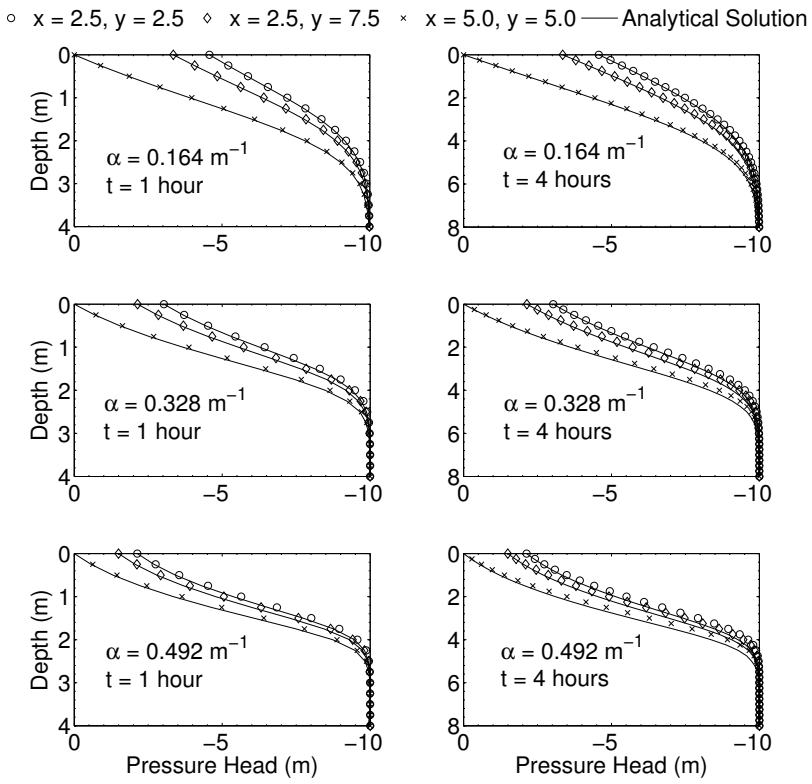

Figure 13: 3D unsaturated flow test case. Distribution of the pressure head versus depth at 1 and 4 h experiment advancement time, for different profiles and for different values of α.

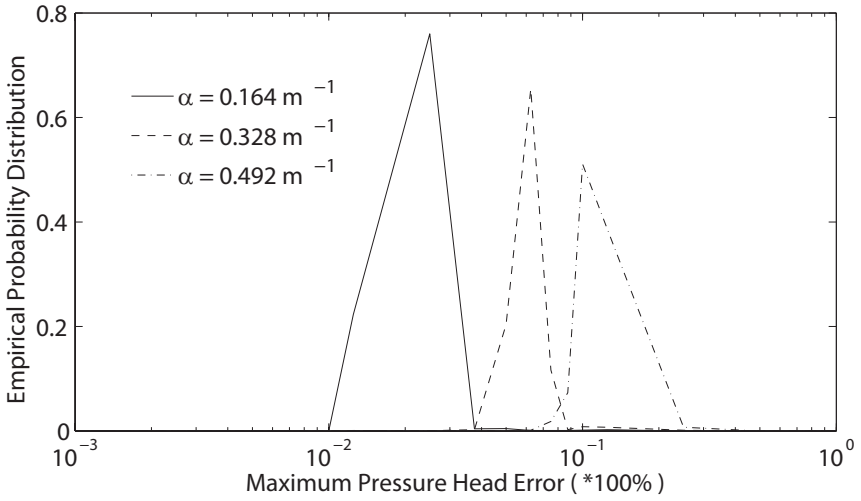

Figure 14: 3D unsaturated flow test case. Empirical probability distribution of the maximum pressure head error for different values of α.

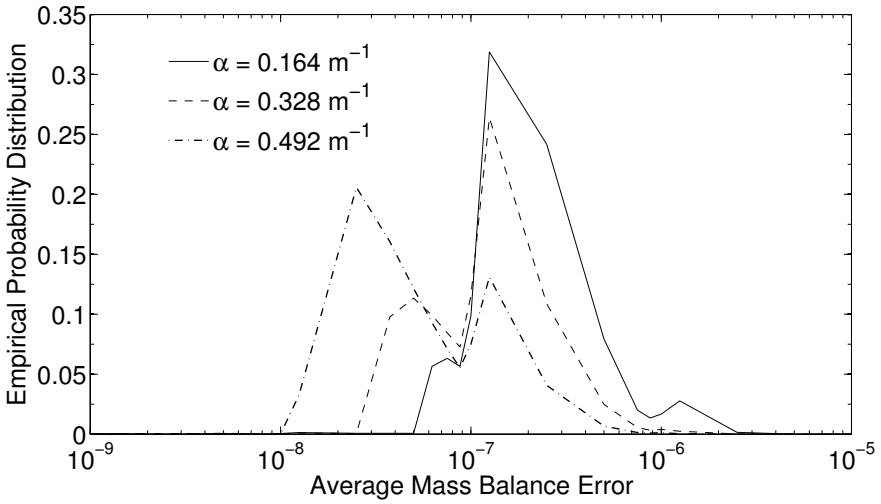

Figure 15: 3D unsaturated flow test case. Empirical probability distribution of the average mass balance error for different values of α.

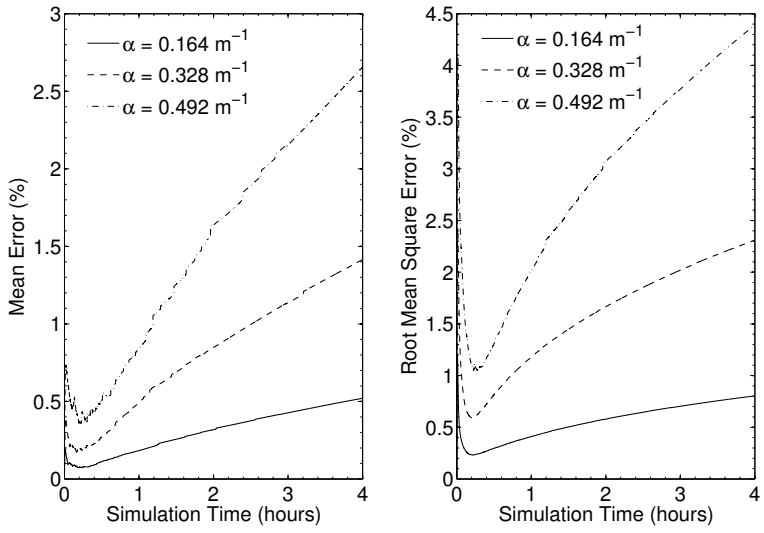

Figure 16: 3D unsaturated flow test case. Evolution of mean average error and root mean square error with time for different values of α.

List of Tables

h**(pressure) - based form:**	$C(h)\frac{\partial h}{\partial t} = \nabla[K(h)\nabla h] + \frac{\partial K(h)}{\partial z}$
θ**(saturation) - based form:**	$\frac{\partial \theta}{\partial t} = \nabla[D(\theta)\nabla \theta] + \frac{\partial K(\theta)}{\partial z}$
The mixed $h - \theta$ **- based form:**	$\frac{\partial \theta}{\partial t} = \nabla[K(h)\nabla h] + \frac{\partial K(h)}{\partial z}$

Table 1: Forms of the Richards' equation that are used as a basis in numerical algorithms

	Infiltration Experiment	Drainage Experiment
$\mathbf{K_{sat}}$ **(m/d)**	8.4	9.6
$\boldsymbol{\theta_s}$	0.3	0.3
$\boldsymbol{\theta_r}$	0.033	0.0
$\boldsymbol{\alpha}$ $\boldsymbol{(m^{-1})}$	3.3	2.98
n	4.1	3.49

Table 2: Soil hydraulic parameters for the simulation of the infiltration and drainage experiment by Vauclin et al. (1975, 1979)

	Berino loamy fine sand	**Glendale clay loam**
$\mathbf{K_{sat}}$ **(m/d)**	5.41	0.131
$\boldsymbol{\theta_s}$	0.3658	0.4686
$\boldsymbol{\theta_r}$	0.0286	0.1060
$\boldsymbol{\alpha}$ $\boldsymbol{(m^{-1})}$	2.8	1.04
n	2.239	1.3954

Table 3: Soil hydraulic parameters for simulation of the heterogeneous soil flow test problems by Kirkland et al. (1992)